Eur. J. Biochem. *254*, 610−619 (1998)

NMR investigation of the multidrug transporter EmrE, an integral membrane protein

Manfred SCHWAIGER[1], Mario LEBENDIKER[2], Hagit YERUSHALMI[2], Murray COLES[1], Adriane GRÖGER[1], Christian SCHWARZ[1], Shimon SCHULDINER[2] and Horst KESSLER[1]

[1] Institut für Organische Chemie und Biochemie, Technische Universität München, Germany
[2] Institute of Life Sciences, Hebrew University of Jerusalem, Israel

(Received 13 February/7 April 1998) − EJB 98 0219/3

EmrE is an *Escherichia coli* multidrug transport protein that confers resistance to a wide range of toxicants by active transport across the bacterial cell membrane. The highly hydrophobic polytopic integral membrane protein has been purified and studied in its full-length form by high-resolution NMR spectroscopy in a mixture of chloroform/methanol/water (6:6:1, by vol.). Full activity is maintained after reconstitution of the protein into proteoliposomes from this solvent mixture. A series of heteronuclear (^{1}H-^{15}N) two- and three-dimensional experiments, as well as triple resonance experiments, were applied to the 110-residue protein and led to the assignment of the ^{1}H, ^{15}N and a large part of the ^{13}C backbone resonances as well as many of the sidechain resonances. A preliminary analysis of the secondary structure, based on sequential NOE connectivities, deviation of chemical shifts from random coil values and $^3J_{NH\text{-}H\alpha}$ coupling constants supports a model where the protein forms four α-helices between residues 4−26 (TM1), 32−53 (TM2), 58−76 (TM3) and 85−106 (TM4). For the residues of helices TM2 and TM3 a significant line broadening occurs due to slow conformational processes.

Keywords: EmrE protein; NMR; membrane protein; multidrug resistance; secondary structure.

Transporters are essential for creating and maintaining the different composition of the cell interior relative to the exterior. They are essential in sustaining life and for adaptation to changes in the environment. In humans their malfunction results in diseases, e.g. cystic fibrosis and cystinuria and they can also be responsible for the failures in drug therapy, e.g. multidrug transporters can be responsible for the difficulties encountered in cancer chemotherapy and for resistance of microorganisms to antibiotics.

The next crucial step in the study of the function of such transporters requires high-resolution structural information which is, as yet, not available. Elucidation of their structures and relating structural and functional information presents a major challenge to the biochemist and the structural biologist and is of utmost importance for the development of transport inhibitors for clinical applications. There are inherent problems in growth of crystals from membrane proteins as they are often only soluble in detergent solution. The detergent covers the hydrophobic regions of the membrane protein surface, while the polar regions, needed for the protein−protein contacts which establish a three-dimensional crystal lattice, are small and also partly covered by detergent. In addition, it has been suggested that adoption of multiple conformations is needed for proper translocation of substrates by transport proteins, a phenomenon which is not easily accessible to X-ray crystallography.

The introduction of NMR spectroscopy as an alternative method for protein structure determination at atomic resolution has led to a significant increase in the number of known protein structures [1]. In addition to providing structural information, NMR has emerged as a powerful method for the study of protein dynamics, an understanding of which is valuable in attempting to correlate structure with function. Three- and four-dimensional heteronuclear NMR spectroscopy of isotopically labeled samples make it possible to study proteins of molecular masses up to 30 kDa and more (for reviews see [2, 3]). However, to date it has only been possible to subject a few integral membrane proteins to NMR analysis, e.g. the subunit c of F_1F_2 ATP synthase [4−7], bacteriophage IKe major coat protein [8] and fragments of bacteriorhodopsin [9, 10]. Very few membrane proteins can be studied by high-resolution NMR, partly because of their size, but above all because of the size of the detergent micelles needed for solubilization (for reviews see [11, 12]). The optimization of solvent conditions also presents a major challenge [13]. Another attempt is to study membrane proteins under anisotropic conditions like oriented lipid bilayers [12, 14, 15] or bicelles [16−18], giving information about the orientation of the protein to the membrane [19].

Here we describe a different approach to the study of EmrE, an H^+-coupled multidrug antiporter from *Escherichia coli* of only 110 amino acids which is soluble in a mixture of organic solvents [20]. Full activity is recovered after reconstitution of the protein from the organic solvents into proteoliposomes [21]. An NMR study in a very similar solvent system has been recently carried out with subunit c of the F_1F_0 ATPase [4−7]. The F_0 complex, which provides a translocation pathway for H^+, is

Correspondence to H. Kessler, Institut für Organische Chemie und Biochemie, Technische Universität München, Lichtenbergstrasse 4, D-85747 Garching, Germany
Fax: +49 89 28913210.
E-mail: kessler@artus.org.chemie.tu-muenchen.de
URL: http://www.org.chemie.tu-muenchen.de

Abbreviations. 2D and 3D, two- and three-dimensional; EmrE, *Escherichia coli* multidrug resistance protein E; HSQC, heteronuclear single-quantum coherence; T_2, transverse relaxation time; TM, putative transmembrane helix; Myr$_2$Gro*P*Cho, dimyristoylglycerophosphocholine; solvent A, chloroform/methanol (1:1, by vol.).

a heterooligomer composed of two other polypeptides (subunits a and b) and about 10−12 copies of subunit c. The structure of monomeric subunit c has been determined in organic solvents as two antiparallel α-helices [7] and it was shown that the protein was folded in a way which retains biochemical properties observed in the native F_0 complex [5].

EmrE is a homooligomer that confers resistance to a wide variety of toxicants by actively removing them from the cell in exchange for protons [20−22]. It is a highly hydrophobic 12-kDa protein which has been purified taking advantage of its unique solubility profile in organic solvents. Hydrophobicity analysis of the sequence yielded four putative transmembrane domains of similar sizes [20]. Results from transmission Fourier-transform infrared measurements agree well with this hypothesis and yielded α-helical estimates of 78% and 80% for EmrE in chloroform/methanol and dimyristoylglycerophosphocholine ($Myr_2GroPCho$), respectively [23]. Furthermore, the fact that most of the amide groups in the membrane-bound protein do not undergo amide proton H/D exchange implies that most (≈80%) of the residues are embedded in the bilayer.

Here we report the overexpression and purification of EmrE and the assignment of the ^1H, ^{15}N and a large part of the ^{13}C backbone resonances as well as many of the sidechain resonances from a series of ^{13}C or ^{15}N edited 3D spectra. The analysis of the secondary structure is based on the NOE pattern of the ^{15}N NOESY-HSQC spectra, HN, Hα, Cα and C=O chemical shifts and $^3J_{NH\text{-}H\alpha}$ coupling constants.

MATERIALS AND METHODS

Cell growth, induction and preparation of membranes. *Escherichia coli* TA15 I^Q cells bearing plasmid pKK56 [21] were grown in minimal medium A supplemented with thiamin (2.5 μg/ml), ampicillin (0.1 mg/ml) and glycerol (0.5%) in 12-l batches. These cells are auxotrophs in which *emrE* is under control of the *tac* promoter in an I^Q background. Cells were grown at 37°C to an $A_{600\,nm}$ of about 0.7−0.9 and isopropyl β-D-thiogalactopyranoside was then added to a final concentration of 0.5 mM. After 2 h, cells were collected by centrifugation and washed in lysis buffer (250 mM sucrose, 150 mM choline chloride, 10 mM Tris/HCl pH 7.5, 0.5 mM dithiothreitol and 2.5 mM $MgSO_4$). At this stage the cell pellets can be kept at −70°C until further processing. For preparation of membrane vesicles, the cells were thawed and resuspended in lysis buffer (6 ml/g wet mass) containing DNase I at 15 μg/ml. The cells were broken up by two passages through a French press at 138 MPa. The membrane vesicles (together with a small percentage of unbroken cells and cell debris) were then sedimented by centrifugation at 210000 *g* for 90 min at 4°C. The pellet was resuspended in lysis buffer to a concentration of 10 mg protein/ml (approximately 1.5 ml/g wet cells). The membrane suspension can be kept at −70°C till further processing.

For ^{15}N-labeling of EmrE the ammonium sulfate in the growth medium was replaced with [^{15}N]ammonium sulfate (Sigma Chemical Co.) at 0.29 g/l. For labeling also with ^{13}C, glycerol was replaced with D-[$^{13}C_6$]glucose (Martek Biosciences Co.) at 0.9 g/l. When labeling with deuterium, the medium was prepared in 75% deuterated water (Martek Biosciences Co.). Cell growth was half that in unlabeled medium and the yield of EmrE also about half.

Extraction of EmrE with chloroform/methanol. For selective extraction of EmrE, the membranes were extracted with a mixture of chloroform and methanol. To allow for rapid detection of EmrE in the various fractions, tracer amounts of [^{35}S]methionine-labeled EmrE, prepared from cells labeled as previously described [21], were added. To 30 ml membrane suspension, 120 μl membranes containing [^{35}S]EmrE (3.4 μg protein/ml, 28000 cpm/μl) was added. Extraction was performed by addition of 500 ml chloroform/methanol (1:1; solvent A) in a 2-l separatory funnel. After thorough mixing, the suspension was kept for 15 min at 4°C, an additional aliquot of 100 ml water was added and kept for another 10 min. Finally 250 ml solvent A were added, followed by mixing and by an additional aliquot of 50 ml water. The mixture was incubated at room temperature until the organic lower phase became completely clear. The lower phase (about 400 ml), containing partially purified EmrE, was collected and stored at room temperature.

Purification of EmrE on hydroxyapatite. To allow for binding of EmrE to the resin, methanol (0.5 vol.) was added to the extract. The hydroxyapatite column was prepared from about 5 g resin (High resolution, Calbiochem) which results in a 20-ml column (2.5 cm width). The column was washed with 4 vol. of each of the following solvents: chloroform/methanol/water (3:3:1); pure methanol; pure chloroform; chloroform/methanol (2:1); chloroform/methanol (1:2). The extract was loaded on the column at low flow rate, and the column was immediately washed with 2 vol. chloroform/methanol (1:2, then 2:1, finally 1:2). EmrE was eluted with 3 vol. chloroform/methanol/water (3:3:1). Fractions were collected and radioactivity was measured. Appropriate fractions were pooled and kept at −70°C.

Delipidation on a Sephadex LH20 size-exclusion column. About 80 g LH-20 lipophilic Sephadex (Pharmacia Biotech) were resuspended and washed with solvent A. The resin was used in a reusable 400-ml column (90.5×2.5 cm). The column was kept in solvent A and reequilibrated with 1 l solvent prior to use. The pool from the hydroxyapatite column (up to 20 ml) was loaded on the Sephadex LH-20 and eluted with solvent A at a flow rate of 2 ml/min. As estimated from radioactivity, EmrE typically eluted in the fractions between 140−180 ml. Phospholipids were qualitatively estimated using Primulin (Sigma Chemicals Co.) for detection on TLC plates with dioleoyl-L-glycerophosphoethanolamine as a standard. The main phospholipid peak started to elute at around 300 ml but a small amount (about 5% of the total lipid) always eluted with EmrE. The proper fractions were pooled and kept at −70°C until further processing. For drying, the sample was kept in a 30°C water bath and dried with a gentle stream of argon to about 0.1 vol. If turbidity developed during drying, a few drops of chloroform were added. At this stage the sample was transferred to 1.5-ml Eppendorf tubes and the drying process was continued, adding chloroform as needed to prevent turbidity. The final 0.5 ml was dried on a speedvac to complete dryness. The sample was kept at −70°C.

SDS/PAGE. For analysis of EmrE in SDS/PAGE, the solvent was dried and the protein was resuspended in sample buffer and analyzed in 16% gels as described [24].

Protein determination. This was performed essentially as described in [25].

NMR experiments. All 3D NMR experiments were performed at 300 K on a four-channel Bruker DMX750 spectrometer, equipped with pulsed-field gradient accessory and a triple resonance probe. Some spectra for optimizing sample conditions were recorded on a similarly equipped Bruker DMX600. Proton chemical shifts were referenced to internal tetramethylsilane, nitrogen and carbon chemical shifts in terms of the frequency ratio Ξ [26]. Carrier positions used were 116.5 (^{15}N), 175.0 (^{13}C=O), 56.0 ($^{13}C\alpha$), 41.0 ($^{13}C\alpha/\beta$) and 4.75 ppm (^1H). In all 2D and 3D experiments with amide proton detection, pulsed-field gradients were used for coherence pathway selection with sensitivity enhancement [27, 28] using the echo/antiecho technique [29, 30]. The numbers of complex points and sweep widths in the

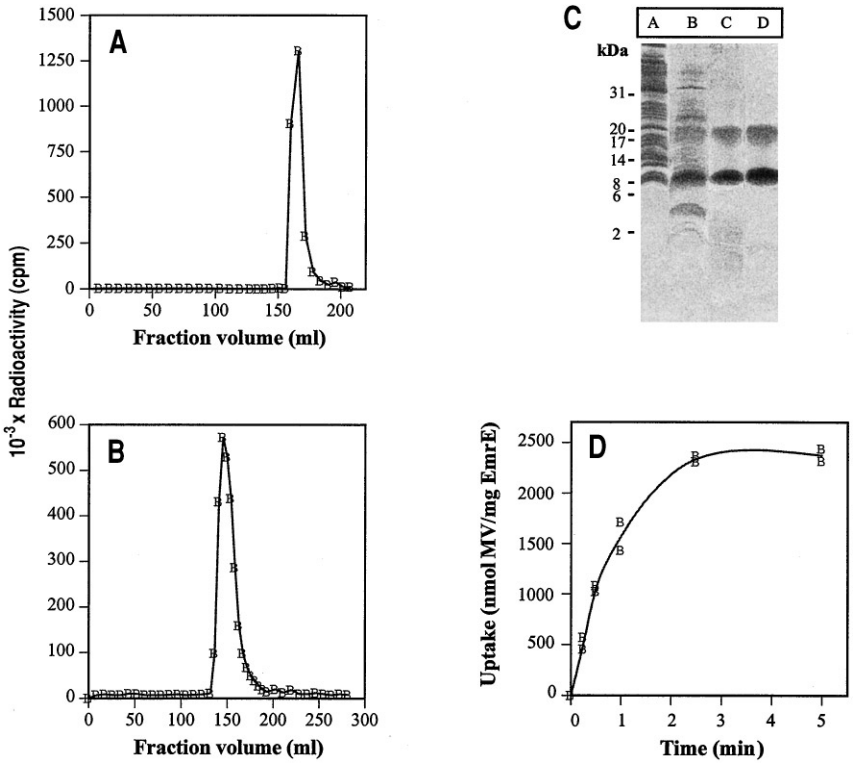

Fig. 1. Purification of EmrE. (A) Hydroxyapatite column. After loading the extract, the column was washed with 140 ml of various mixtures of chloroform and methanol as described under Materials and Methods. At this point elution was performed with a mixture of chloroform/methanol/water (3:3:1). The three fractions with the highest radioactivity were pooled. The shoulder with about 10% of the radioactivity was discarded because of the impurities it contained. (B) Sephadex LH20: The lipophilic Sephadex was used to delipidate EmrE. The peak of the lipids in this column was detected starting at 190 ml. (C) SDS/PAGE analysis of different stages of purification. Lane A, total membranes (10 μg protein) after induction with isopropyl *β*-D-thiogalactopyranoside; lane B, chloroform/methanol extract of above membranes containing 1 μg EmrE as estimated from radioactivity levels; lane C, EmrE (1 μg) after purification on hydroxyapatite (the small amount of polypeptide with a larger apparent molecular mass is a dimer of EmrE, as judged from the fact that it is also labeled with [^{35}S]methionine; this aggregation in SDS/PAGE is typical of membrane proteins and is increased if the sample is boiled); lane D, EmrE (1 μg) after delipidation on a Sephadex LH20 column. (D) Transport of [^{14}C]methyl viologen: Proteoliposomes containing 0.19 M NH_4Cl and reconstituted with purified EmrE (270 ng/reaction) were diluted into an ammonium-free medium and assayed as previously described [21].

amide dimensions were 512 points/12.0 ppm for ^{1}H and 46 points/25.0 ppm for ^{15}N (unless otherwise noted). Quadrature detection in the other indirectly detected dimension was accomplished using the States-TPPI method [33]. The ^{15}N dimension in the HNCA, HNCO, H(CCO)NH and C(CCO)NH experiments was recorded in a constant-time manner [31].

The following numbers of complex points and sweep widths were employed in the experiments used in the present study: 2D ^{1}H-^{15}N-HSQC with water flipback [32], ^{15}N (F_1) 256 points/25.0 ppm, NH (F_2) 512 points/12.0 ppm (16 transients); TOCSY-HSQC [33] with a 60-ms DIPSI-2 mixing period [34], ^{1}H (F_2) 72 points/12.0 ppm (16 transients); NOESY-HSQC with mixing times of 40 ms and 100 ms [35, 36], ^{1}H (F_2) 100 points/12.0 ppm (16 transients); HNHA [37], ^{15}N (F_1) 20 points/25.0 ppm, ^{1}H (F_2) 90 points/12.0 ppm (32 transients); HNHB [38], ^{1}H (F_1) 40 points/12.0 ppm (32 transients). All of these experiments were recorded on uniformly ^{15}N-labeled samples, whereas uniformly ^{13}C/^{15}N-labeled samples were used for: CT-HNCA [39], ^{13}C (F_1) 56 points/26 ppm (16 transients); CT-HNCO [39] ^{13}C (F_1) 76 points/16 ppm (8 transients); HCCH-TOCSY [40], ^{13}C (F_1) 56 points/36.5 ppm, ^{1}H (F_2) 74 points/5.5 ppm ^{1}H (F_3) 512 points/7.0 ppm (32 transients). A 75% deuterated uniformly ^{13}C/^{15}N-labeled protein sample was used to record a C(CCO)NH [41] experiment [^{13}C (F_1) 45 points/60 ppm (64 transients)] and an H(CCO)NH [42] experiment [^{1}H (F_1) 48 points/12 ppm (64 transients)]. Additionally a 2D NOESY spectrum with WATERGATE [43] water suppression was recorded with an unlabeled protein sample ^{1}H (F_1) 925 points/12 ppm; ^{1}H (F_2) 2048 points/12 ppm (128 transients). $^3J_{NH\text{-}H\alpha}$ coupling constants were determined from the HNHA spectrum as described in [37].

Heteronuclear ^{15}N{^{1}H} NOEs were measured using the pulse sequence of Barbato et al. [44]. In this set of experiments one spectrum was acquired with 3-s proton presaturation (i.e. no ^{15}N{^{1}H}-NOE build-up) and another spectrum was acquired without proton presaturation for reference. Both experiments were repeated and the results were averaged to reduce the experimental error. NMR spectra were processed using the programs UXNMR and AURELIA (Bruker) and the software package SYBYL (Tripos Associates, Inc.). For the indirect dimensions linear prediction, zero filling to the next power of 2 and apodization with a 90°-shifted squared sine bell were used. In the direct dimension zero filling to 1024 points, apodization with a 60°-shifted squared sine bell and baseline correction were applied.

RESULTS

Overproduction and purification of EmrE. The overproduction step and the selective extraction with organic solvents are crucial for purification of EmrE to homogeneity. As with most, if not all, membrane proteins, overproduction of EmrE inhibits cell growth. Therefore, a tightly regulated expression system has been used. This system is based on the *tac* promoter in a cell

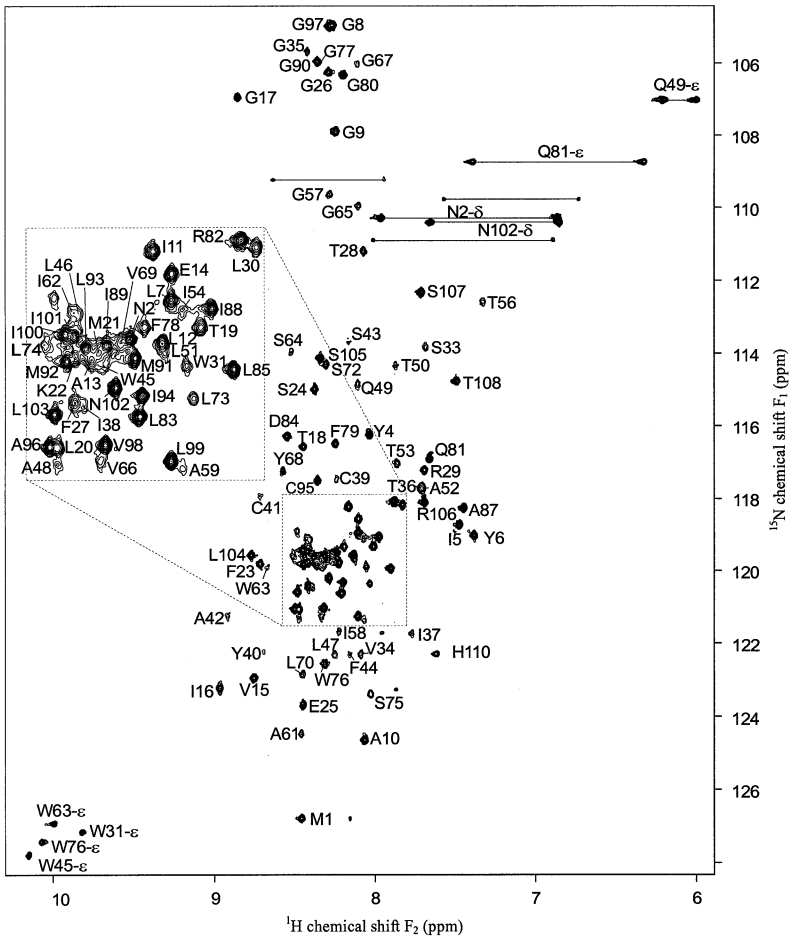

Fig. 2. 750-MHz ^{1}H-^{15}N-HSQC spectrum of EmrE. A 1-mM solution of [U-^{15}N]EmrE in $CDCl_3/CD_3OH/H_2O$ (6:6:1, by vol.) plus 200 mM ammonium acetate (pH 6.2) at 27°C was used. The assignments for the amide proton−nitrogen pairs are indicated. Sidechain amino group signals are marked by horizontal lines. The highly overlapped region in the center of the spectrum has been enlarged in the dotted zoomed box.

Table 1. Purification of EmrE. The amount of radioactivity in whole cells was estimated after precipitation with ice-cold trichloroacetic acid (5%). Other detais are explained in the text.

Fraction	Volume	[^{35}S]Methionine	Protein	Specific activity	Yield	Purification
	ml	cpm	mg	cpm/mg protein	%	-fold
Cells		1.5×10^{6}	3500	428	100	1
Membranes	17.0	1.2×10^{6}	320	3750	80	8.8
Chloroform/methanol extract	340.0	1.0×10^{6}	12.4	80645	67	188
Hydroxyapatite	16.8	0.9×10^{6}	8.3	108400	60	253
Sephadex LH-20	23.5	0.8×10^{6}	7.6	105300	53	245

expressing the *lac* I^{Q} repressor. Under uninduced conditions the background expression is very low and the levels of EmrE are undetectable [21]. Upon induction, cells stop growing and high levels of EmrE are detected after 2 h as visualized on Coomassie-blue stained gels after differential extraction with chloroform/methanol (Fig. 1C, lane B). EmrE is differentially extracted with this solvent mixture and, therefore, highly purified (compare with membranes in Fig. 1C, lane A). Using EmrE specifically labeled with [^{35}S]methionine, we have estimated the efficiency of extraction to be approximatly 80% (Table 1). The total amount of membrane proteins extracted is less than 4% and, therefore, a purification of more than 20-fold is obtained in this step yielding a highly enriched preparation. To remove minor impurities, EmrE was allowed to bind to a hydroxyapatite column. Binding to this column was very efficient and EmrE was not released during thorough washings with various chloroform/methanol mixtures (Fig. 1A). When a small amount of water was added to the solvent mixture, a rapid and quantitative elution of EmrE was detected. The main peak was collected but special care was taken not to include the last 10% of the peak, since it contained a number of impurities such as a small peptide with an apparent molecular mass of 4 kDa and a polypeptide with a mobility slightly lower than EmrE. At this stage, EmrE is homogeneous and pure as determined from amino-acid sequencing of this preparation and, as will be seen below, from analysis of the NMR spectra. For easier handling of the sample and to avoid possible interference in the NMR spectra, we removed the majority of the lipids associated with EmrE. This was

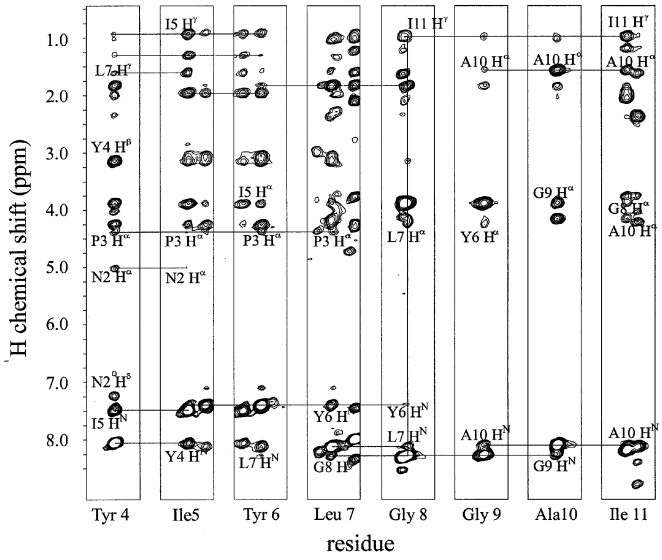

Fig. 3. Selected strips of the ^{15}N-edited 3D NOESY spectrum, indicating the sequential assignment pathway. Sequential peaks are connected by lines. The sequential assignment was based mainly on $d_{NN}(i,i+1)$ NOEs. In case of ambiguity or overlap, the whole pattern of sidechain resonances was considered.

achieved with a size-exclusion column, Sephadex LH-20, and the results are shown in Fig. 1B. In this step, EmrE eluted very close to the void volume while the bulk of the phospholipids were retarded enough to allow for separation without significant loss of material (85% yield in this step, see Table 1). The peak containing EmrE was dried down as described under Materials and Methods taking the precautions described in detail previously [45]. At this stage, purified EmrE was reconstituted in membrane vesicles and tested for ΔpH-dependent [^{14}C]methyl viologen uptake. Rates of about 800−1500 nmol · min^{-1} · mg protein^{-1} (at pH 8.5, methyl viologen concentration of 18.75 μM) were observed (for an example see Fig. 1D).

Sample preparation. Our initial NMR experiments were designed to optimize protein solubility at the concentrations and temperatures required for recording NMR spectra. Achieving reproducible solubility and stability at these concentrations was difficult and required some compromises. Several uniformly ^{15}N-labeled samples were prepared to optimize the conditions with respect to sample stability, resolution and signal intensity by recording ^{15}N-HSQC spectra. Various solvent mixtures, pH, salt composition and concentrations were tested. Finally stable protein concentrations as high as 15 mg/ml have been achieved in a mixture of chloroform/methanol/water (6:6:1, by vol.) including 200 mM ammonium acetate pH 6.2. During all sample manipulations, we observed a loss of signal intensity for the ^{15}N-HSQC peaks with every step, even for samples kept at experimental conditions. After a few weeks, NMR signals are no longer observable and the sample shows no biological activity, although no visible precipitation occurs and the protein seems to be completely dissolved. The signals in the ^{15}N-HSQC spectrum vanish within several days without changing their shape or position and without any new resonances appearing. By optimizing the sample conditions, we managed to slow down this process sufficiently to give us almost stable sample conditions for the duration of an NMR experiment. In general, every sample could be used for recording NMR spectra for a term of one or two weeks. This is quite a short time for an NMR structure determination, but it is sufficient to record 2D and 3D spectra. Fresh samples were used when the old ones deteriorated as judged from the decrease in the intensity of the signals in the ^{15}N-HSQC spectrum.

Special spectral features. The chemical shift dispersion of the NMR resonances of EmrE is very poor and many signals are highly overlapped. The amide proton resonances, for example, are confined to a spectral region of only 1.7 ppm, extending over 7.3−9.0 ppm. Also, all but one of the Hα protons resonate in the small spectral range of 3.6−4.7 ppm. Obtaining the highest possible resolution was therefore crucial for success in the NMR work, as was a careful optimization of every step in the processing of the spectra. To achieve a maximum resolution as well as sensitivity, we recorded almost all spectra at 750 MHz.

Fig. 2 shows the ^{15}N-HSQC spectrum of [U-^{15}N]EmrE. Many signals overlap, especially in the small region 118−121.5 ppm in F_1 and 7.8−8.5 ppm in F_2 that contains about 40% of the backbone amide resonances. In addition, a substantial variation in line width and peak intensity is apparent in this spectrum. The broad and very weak NMR signals were later assigned to residues 31−75 (helices TM2 and TM3), whereas the rest of the residues show sharp signals of high intensity. No TOCSY cross-peaks were observed for the residues with weak, broad signals and their signal intensity in all other spectra was also very low.

Assignment strategy. Only 60% of the expected residues were observed in the ^{15}N-TOCSY-HSQC spectrum. For most other residues giving rise to a signal in the ^{15}N-HSQC, not even diagonal peaks were visible in the 3D-TOCSY. On the other hand, each of the 105 amide protons showed several cross-peaks in the ^{15}N-NOESY-HSQC spectra, although with significantly lower intensity for those residues which showed no peaks in the TOCSY spectrum. Because of the lack of information, we were not able to perform the sequential assignment from these two spectra according to the commonly used strategy [46].

To circumvent these problems, we recorded an HNHA spectrum, known to be less sensitive to chemical exchange processes than experiments based on the TOCSY transfer. The cross-peak intensity in an HNHA spectrum depends on the $^3J_{NH\text{-}H\alpha}$ coupling constants which are expected to be comparatively low for residues in helices, and on the HSQC peak intensity. Nevertheless all of the residues of the problematic helices showed cross-peaks in this spectrum, although some were very weak. Based on this data, we were able to assign all Hα proton resonances. Also more than 90% of the Hβ protons could be assigned from an HNHB spectrum. Sequence-specific assignment of spin systems was achieved using interresidual NOEs. Due to the highly helical nature of the protein, the ^{15}N-NOESY-HSQC spectrum shows a large number of $d_{NN}(i,i+1)$ connectivities between sequential amides, although many of them overlap. Ambiguities due to overlapping or low-intensity signals were reduced by careful inspection of the whole NOE pattern, taking into account the large number of $d_{\alpha N}(i,i+1)$ and $d_{\alpha N}(i,i+3)$ connectivities as well as NOEs from amide protons to sidechain protons of adjacent amino acids, as shown in Fig. 3. Additionally the spin systems and typical chemical shifts of some amino acids, such as glycine and alanine, were taken into account in comparison with their known position in the protein sequence. Based on this strategy, it was possible to achieve complete sequential assignment for all residues with exception of proline.

Assignment of backbone ^{13}C resonances was attempted in order to allow comparison of Cα and C=O chemical shifts to random coil values. In addition, assignment of both backbone and sidechain ^{13}C resonances would allow the analysis of ^{13}C-edited NOESY spectra. Such spectra would be very helpful for

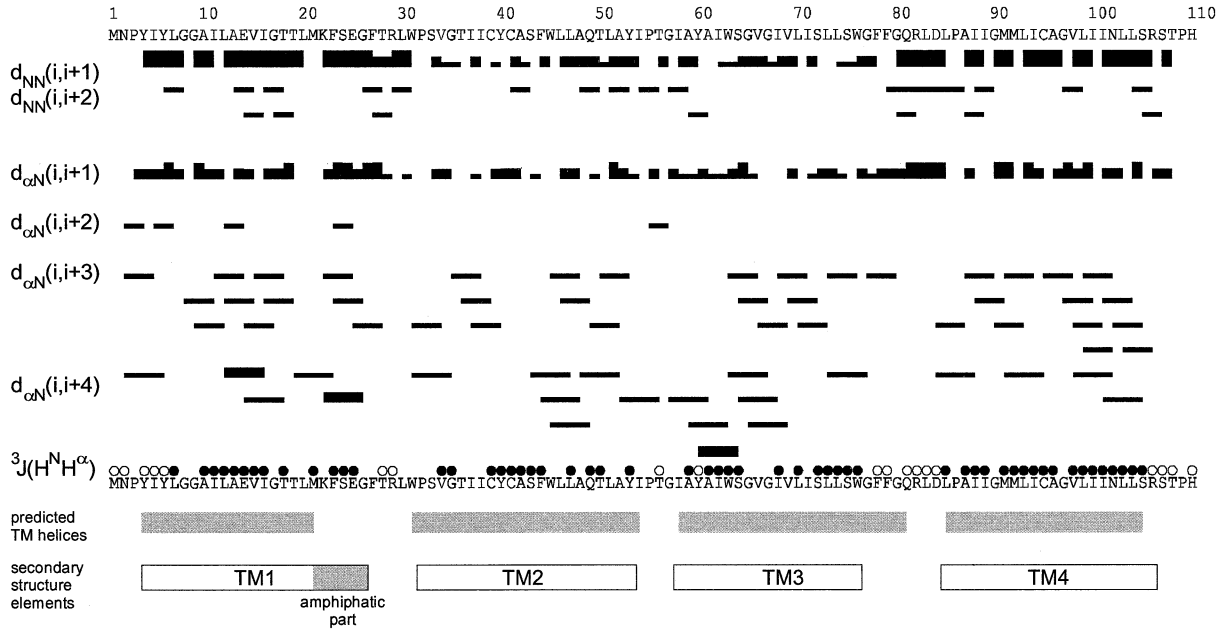

Fig. 4. Summary of the sequential and medium-range NOE connectivities and $^3J_{NH\text{-}H\alpha}$ coupling constants for EmrE. NOE signals typical for α-helical proteins are shown. (●) $^3J_{NH\text{-}H\alpha} < 4.5$ Hz; (○) $^3J_{NH\text{-}H\alpha} > 4.5$ Hz. The results of the hydrophobicity analysis are also listed, and position of the helices determined in this study marked as TM1−TM4. The previously predicted helical regions do not completely match the helical assignments based upon our NMR results, especially for helix TM1, which has an additional amphipathic part.

achieving additional structural information, especially for evaluation of interhelical long-range contacts. In order to achieve an assignment for the backbone ^{13}C resonances, we recorded a 3D HNCO and a 3D HNCA experiment with a uniformly $^{13}C/^{15}N$-labeled sample. Unfortunately, in these spectra again we observed only very weak signals for residues of the helices TM2 and TM3. We were therefore able to assign only approximately 80% of the backbone ^{13}C resonances, mainly for the residues of helices TM1 and TM4. The HNCA additionally allowed us to confirm the sequential assignments in cases where an interresidual and a sequential Cα peak were visible. Additional ^1H as well as a partial ^{13}C sidechain assignment was achieved from an HCCH-TOCSY experiment, recorded with a uniformly $^{13}C/^{15}N$-labeled sample and from an H(CCO)NH and a C(CCO)NH spectrum, recorded with a 75% deuterated and uniformly $^{13}C/^{15}N$-labeled sample.

Evaluation of secondary structure. Information about secondary structure from NMR data can be obtained from a qualitative analysis of NOE interactions and $^3J_{NH\text{-}H\alpha}$ coupling constants [46]. Fig. 4 summarises the observed NOE connectivities and coupling constants for EmrE. A specific pattern of sequential and medium-range NOE cross-peaks and coupling constant characteristic of α-helices is observed, i.e. strong $d_{NN}(i,i+1)$, $d_{\alpha N}(i,i+3)$ and in some cases $d_{\alpha\beta}(i,i+3)$ and $d_{\alpha N}(i,i+4)$ NOEs and $^3J_{NH\text{-}H\alpha}$ coupling constants below 4.5 Hz. This pattern defines four helices of approximately equal length, and can be established despite the overlap of many signals. In fact, more problems were encountered in characterising the loop or turn regions between the helices.

Secondary structure elements are commonly confirmed by characteristic deviations of backbone ^1H and ^{13}C chemical shifts from their random coil values [47, 48]. However, available random coil chemical shifts have been obtained from reference peptides and proteins dissolved in water. As chemical shifts strongly depend on solvent conditions, we developed our own shift reference measuring the peptides (Boc-Gly-Gly-Xaa-Leu-Gly-Me) in chloroform/methanol (1:1) (Schwaiger, M., Riemer, C. and Kessler, H., unpublished results). The deviation of chemical shift for the HN, Hα, Cα resonances for EmrE from these values is shown in Fig. 5. As C=O random coil shifts were not determined in this study, we show a comparison with the shift values from [38] in this figure. Amide proton, C=O and especially Cα resonances are shifted upfield, whereas Hα protons are shifted downfield almost throughout the entire sequence, indicating a helical structure. The chemical shift values approach the random coil values at the end of the sequence and in the areas where loops or turns between the helices are expected.

The exact positions of the beginnings and ends of the helices could be determined only from a combination of sequential NOEs, chemical shift information, coupling constants and an extensive consideration of all available NOE connectivities. The first residue of helix TM1 cannot be determined precisely from sequential and medium-range NOE connectivities alone. Due to the extremely high overlap of the Hα residues of Tyr4, Leu7, Gly8, Gly9 and Ala10 it is not possible to assign typical sequential and medium-range NOE connectivities for these residues. The first sequential $d_{\alpha N}(i,i+3)$ NOE that could be assigned unambiguously was from Ile11 to Gly8. Although residues 4−6 show comparatively high coupling constants, inconsistent with a helical secondary structure, the chemical shift deviation clearly indicates that they are part of the helix. Chemical shift deviations also show a disruption in the helix for Gly8 and Gly9, not surprisingly as sequential Gly residues are not likely to participate in an ideal α-helix. Thus it seems likely that the first helix begins at Tyr4, although it may be irregular in nature over its first four residues.

Thr28 is the last residue of TM1. It shows $d_{\alpha N}(i,i+3)$ connectivities to the preceding turn of the helix, especially to Glu25, whereas such signals are missing for the following two residues. TM2 begins at or just after Pro32 as established by $d_{\alpha N}(i,i+3)$ connectivities. The determination of the position of the loop between the helices TM2 and TM3 was difficult, although it is clear that helix TM2 reaches at least to Tyr53. Because of high spectral overlap it was not possible to decide if Ile54 is the last residue of this helix or if it is part of the small loop region

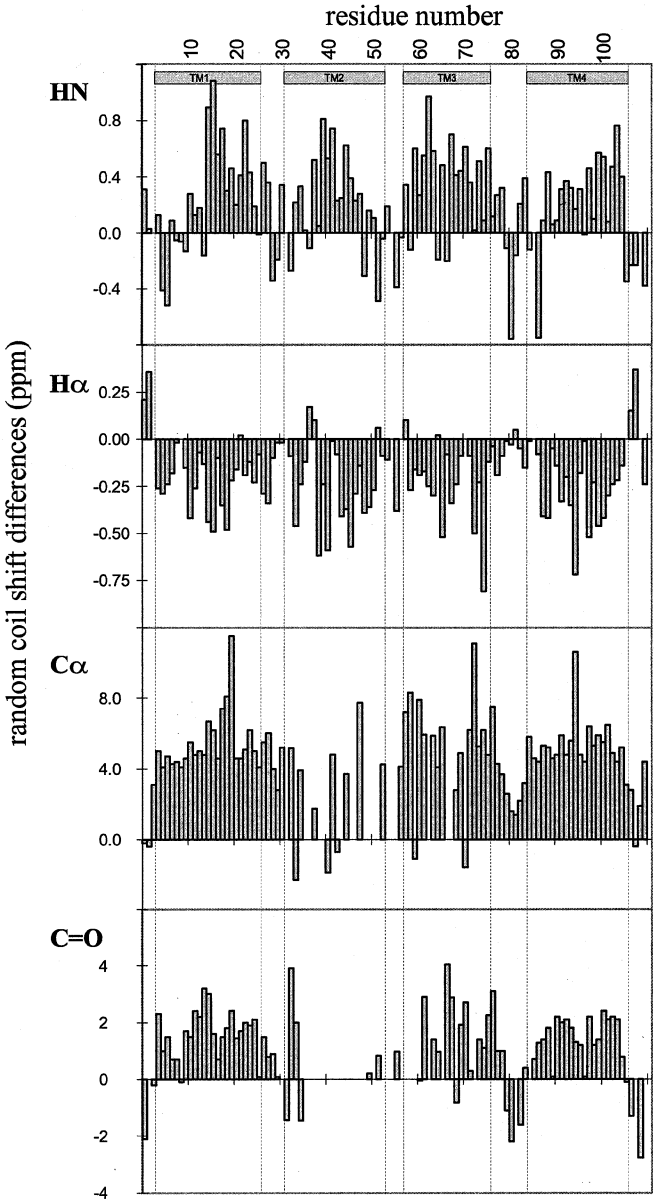

Fig. 5. Chemical shift deviations for backbone HN, H*α*, C*α* resonances from random coil shifts as determined for peptides Boc-Gly-Gly-Xaa-Leu-Gly-Me in chloroform/methanol. For the C=O chemical shifts, the deviation from random coil shifts in water is given, as the corresponding values were not determined for the peptides mentioned above.

between TM2 and TM3. The first $d_{\alpha N}(i,i+3)$ connectivity assigned unambiguously to establish the beginning of TM3 is from Tyr60 to Gly57.

Helix TM3 shows an NOE pattern typical for an α-helix up to residue Trp76. However, Gly77 seems to initiate the transition between a regular α-helix and a looser helical turn, which is connected to a flexible loop region between Gly80 and Asp84. The residues in this region show some NOEs that are strong indicators for helices, i.e. a $d_{\alpha b}(i,i+3)$ NOE between Trp76 and Phe79, whereas others, also expected for an α-helix such as $d_{\alpha N}(i,i+3)$ connectivities between Ser75 and Phe78 and between Leu74 and Gly77, are missing. The last helix is clearly defined and begins at residue Leu85 and ends at residue Ser106. In summarizing, the four helices can be described as follows: 4−26 (TM1), 32−53 (TM2), 58−76 (TM3) and 85−106 (TM4).

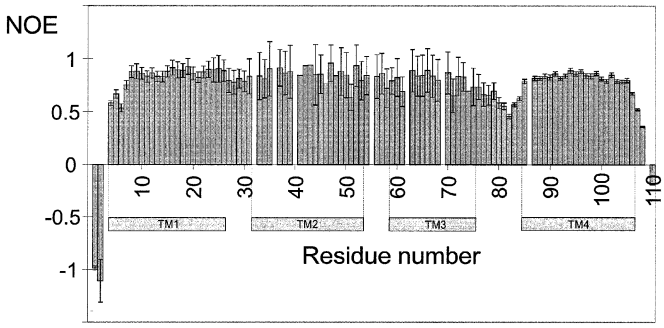

Fig. 6. Plot of the heteronuclear $^{15}N\{^1H\}$-NOE at 76.01 MHz as a function of residue number.

Backbone dynamics. The dynamic behaviour of a protein can be probed by means of heteronuclear $^{15}N\{^1H\}$-NOE and T_1 and T_2 relaxation experiments. While precise relaxation measurements are still in progress, we present here a preliminary discussion of motional behavior based upon a qualitative analysis of ^{15}N heteronuclear NOE measurements at 76.01 MHz ^{15}N frequency, shown in Fig. 6.

As shown the $^{15}N\{^1H\}$-NOE approaches its theoretical maximum value for all transmembrane helices (TM1−4), indicating that these secondary structure elements are not flexible on a time scale faster than 2 ns. Although signal intensities for TM2 and TM3 generally are very low and the derived $^{15}N\{^1H\}$-NOE values are consequently subject to rather high errors, Fig. 6 still shows that they cannot lie far below their theoretical maximum value. In contrast, the $^{15}N\{^1H\}$-NOE drops significantly in the loop between TM3 and TM4 and even becomes negative towards the C- and N-terminal residues, indicating motional flexibility for these regions on an intermediate time scale between 2 ns and the extreme narrowing limit of around 100 ps.

DISCUSSION

Solvent system. First, some remarks should be made on the choice of solubilization medium. In general two alternatives are given for studying membrane proteins in an isotropic environment for obtaining high-resolution NMR spectra: detergent micelles and organic solvents [11]. Detergent micelles are clearly the more favoured media from a biological point of view and they have been applied sucessfully to small membrane-bound proteins and peptides (for examples see [8, 50, 51]). However, the detergents of the micelle largely increase the effective size of the protein, leading to longer molecular correlation times. This restricts the use of detergents to comparatively small proteins, as the largely increased transverse T_2 relaxation diminishes sensitivity of multidimensional NMR experiments.

The use of organic solvents as a membrane mimetic circumvents these problems and allows an investigation of somewhat larger proteins by well known solution NMR methods. Though this approach has been used successfully in studies of peptide sequences of bacteriorhodopsin [9] and on subunit c of F_1F_0 ATP synthase [4−6], their use is still controversial. It is well known that solvent systems like trifluoroethanol/water can induce or stabilize helices [52], disturb tertiary contacts and induce nonnative conformations [53] under unfavourable conditions. The use of organic solvent systems will therefore not be generally applicable to all integral membrane proteins, especially in cases where substantial hydrophilic domains are present in addition to the apolar transmembrane sequences, and solvent conditions have to be adjusted very carefully [13]. However, mixtures of chloroform/methanol, especially if they contain some water, and

certain mixtures of trifluoroethanol/water, seem to provide a proper environment for a native-like folding of some membrane-bound peptides and proteins. Very similar structures were observed in some comparative studies [9, 54, 55] and for subunit c of F_1F_0 ATPase it was shown that the protein is folded in a way which retains biochemical properties observed in the native F_0 complex [5].

We recently studied the properties of chloroform/methanol mixtures by extensive molecular dynamics calculations [56] which exhibited dynamic clustering of the individual solvents. Clusters of about 10 Å are formed at room temperatures and amphiphilic molecules are specifically solvated. The analysis of the molecular dynamics trajecory showed that polar groups are statistically more surrounded by methanol and lipophilic groups by chloroform. These properties of the solvent can explain the solvation of transmembrane proteins. Such solvent mixtures are, for a membrane protein, far more realistic than studies in water and the structure can correspond to the biologically functional molecule as long as there is no specific requirement for an anisotropic environment with polarity separated by nonpolar environment of the thickness of a membrane.

However, it is, in principle, impossible to test the activity of a transport protein in an isotropic environment and therefore provide definite evidence about how well the determined solution conformation represents the protein's native and active form. However, there are some indications for the relevance of the conformation of EmrE in the current solvent system. a) The protein retains biological activity after reconstitution into proteoliposomes and therefore is not irreversibly denatured. Real denaturation of EmrE, which easily occurs with unfavourable solvent conditions, high temperature and sample aging, on the other hand, is an irreversible process. b) The chemical shift values of the backbone protons and carbons show significant and characteristic deviations from the random coil shifts, indicating an α-helical secondary structure. Also a high number of $d_{N\alpha}(i,i+3)$ and $d_{N\alpha}(i,i+4)$ NOEs, as well as small $^3J_{NH\text{-}H\alpha}$ coupling constants confirm the existence of a folded protein. c) It was shown by transmission Fourier-transform infrared experiments that the protein adopts the same highly helical secondary structure both in $Myr_2GroPCho$ vesicles and in the organic solvent mixture [23].

These points emphasize that the protein retains at least the secondary structure present in the native state. Indications that these secondary structure elements are bound together in a compact tertiary structure could be given from long-range NOE contacts or from distance measurements from paramagnetic spin-labeling experiments, as was done for subunit c from F_1F_0 ATP synthase [5]. Because of the extremly high spectral overlap, it has not yet been possible to assign unambiguously such long-range contacts between the helices from the NOESY spectra for EmrE.

Sample conditions and special spectral features. Although the solvent system seems to provide a feasable environment for proper protein folding, no long-term sample stability was achieved over more than one week. As the NMR signals slowly disappear without changing their position and without any new signals appearing, the degenerated protein must form a conformation that is invisible to NMR spectroscopy, but soluble in the solvent mixture. It is well known from the literature that membrane proteins can aggregate under unfavorable conditions and also on sample aging by formation of extensive soluble β-sheet aggregates [57]. This leads to disappearance of the NMR signals as the resonances of the large aggregates are too broad to be seen due to the extremely short T_2 relaxation times [11]. Despite these problems, we were at least able to stabilize the samples sufficiently to allow the acquisition of multidimensional NMR spectra without significant changes in sample conditions during one experiment. This was ensured by recording 2D ^{15}N-HSQC spectra before and after every longer experiment and comparing signal intensities and chemical shift values.

EmrE was expected to have a predominantly α-helical structure [23]. Additionally, due to the highly hydrophobic character of the transmembrane helices, the protein has more hydrophobic and less polar, charged or aromatic residues than typical water-soluble proteins. The low dispersion of chemical shifts and the extremely high spectral overlap observed for EmrE are therefore, for a protein of uniform amino acid composition and secondary structure, not very surprising. Assignment problems are particularly difficult for methyl groups. As they play a crucial role in forming the tertiary contacts between the helices, their assignment would be highly desirable for determination of long-range constraints necessary for a proper structure calculation. The amino-acid composition of EmrE is very rich in a small subset of residue types (Leu, Ile, Val, and Ala), each of them containing one or two methyl groups, leading to a total number of 92 methyl groups. As they all resonate in a very small spectral range, it was impossible to resolve their signals in a conventional ^{13}C-edited spectrum. Multiquantum filtering techniques which select only methyl group resonances allow the detection of a smaller spectral range with a much higher resolution and therefore seemed to provide a solution for this problem. Therefore we developed new pulse sequences for a selective detection of NOEs from methyl groups [58]. Although these experiments are optimized to achieve highest spectral resolution and provide a valuable tool for obtaining structural data for methyl groups in other proteins, it was still impossible to resolve the extremely overlapped methyl resonances of EmrE.

Another problem was that the amide protons of residues TM2 and TM3 show very weak and broad resonances. Possible reasons for line broadening could either be a very long molecular rotational correlation time due to protein oligomerisation or contributions to the transversal relaxation time due to conformational exchange processes. If the line broadening is due to conformational exchange processes, then the line width should depend on the magnetic field strength. This was not observed, nor did we see any improvement upon using HSQC experiments designed to suppress exchange processes [59]. Also the fact that peaks were observed in COSY-type experiments like the HNHA and the HNHB, but not in TOCSY-type experiments argues against conformational exchange broadening. We therefore suspect that the line broadening is due to T_2 relaxation, although to date we cannot explain the big differences in relaxation properties between the particular helices. Up to now accurate T_2 measurements are not available, but big differences in T_2 relaxation could be possible only if overall motions of the molecule are considerably anisotropic. These issues are currently being studied in more detail by relaxation time measurements in various fields.

At this point it is interesting to note that similar processes were observed for the residues of a four-helical bundle of bacteriorhodopsin dissolved in methanol/chloroform (1:1) in a previous study [10] and seem to be an intrinsic property of membrane proteins dissolved in organic solvents.

Secondary structure. Hydrophobicity calculations and theoretical considerations suggest that EmrE consists of four transmembrane helices (residue 4−21, 32−52, 58−79, and 85−106). The results of secondary structure analysis presented in this work are in a general agreement with these predictions, although some significant differences occur, especially for TM1. This helix appears to be longer than predicted, extending to residue 26. It is

interesting to note that the additional part of the TM1 helix (22−26) is amphiphilic, as every third or fourth residue has charged or polar sidechains. TM1 also shows some NOE interactions not typical of a regular α-helix, i.e. the $d_{\alpha N}(i,i+2)$ NOE observed between Leu12 and Glu14. Glu14 is the only charged residue within the transmembrane regions of EmrE and is conserved in all members of the miniTEXANE family. It has been implicated in the H^+ translocation pathway as shown by mutational studies [20]. It is possible that the $d_{\alpha N}(i,i+2)$ connectivity is the result of a kink in the helix which may be significant for the function of the protein. The kink would be expected to result in the helix being partially tilted against the membrane normal. This would also be in agreement with data from Fourier-transfrom infrared measurements which suggest an average helix tilt angle from the bilayer normal of 27° [23].

Another difference from secondary structure predictions occurs at the end of TM3. In contrast to TM1, this helix is somewhat shorter than predicted, ending at residue 76. However, the NMR data show that the following three residues, which are predicted to be part of the helix, form either an irregular helical structure or a helical turn rather than a flexible loop. This disruption to the regular α-helical structure may be caused by Gly77: the heteronuclear NOEs show that residues 77−79 are considerably less flexible than the following residues (78−85) which form the true loop region between TM3 and TM4.

The loop region between TM3 and TM4 is both the longest and most flexible of the interhelical loops. All other helices are connected by very short loops or helical turns which do not appear to be significantly more flexible than the helices themselves. The existence of any recognizable secondary structure elements in these loops is very difficult to determine, not the least because of extensive spectral overlap. However, there are some significant deviations of chemical shifts in these regions from random coil values. It is worth mentioning here that random coil shift differences as determined for this solvent system are in general slightly smaller than those commonly observed for proteins dissolved in aqueous systems. Thus the deviations from random coil values observed for the loops provide further evidence against their extensive flexibility.

The secondary structure reported here is in perfect agreement with a protein topology involving four transmembrane helices. In this case, the short interhelical loops dictate that only an up-down topology is possible. Thus the amphiphatic section of TM1 and the irregular section of TM3 would be expected to be at the same end of the molecule. These two features, together with the possible kink in TM1, may combine to form a recognition site or a funnel-like structure for a charged substrate molecule. However, the tertiary structure could not yet be determined because of high spectral overlap, which hampers assignment of interhelical NOE connectivities, and the broad lines observed for many residues.

Conclusion. In this study we have described the overproduction and purification of EmrE, an *Escherichia coli* multidrug transporter protein. We have successfully assigned the ^1H, ^{15}N and a large part of the ^{13}C backbone resonances as well as many of the side-chain resonances from a series of ^{15}N- and ^{13}C-edited 3D spectra of EmrE in chloroform/methanol/water (6:6:1, by vol.). The analysis of the secondary structure of EmrE in the organic solvent system used proves the existence of four α-helices, ranging over residues 4−26 (TM1), 32−53 (TM2), 58−76 (TM3) and 85−106 (TM4). Helix TM1 contains an amphiphilic part at the C-terminus and NOE analysis indicates that some of the helices are partially kinked.

This work was supported by the *Deutsche Forschungsgemeinschaft*, by the *Fonds der Chemischen Industrie* and by the Israel Science Foundation. The authors would like to thank M. Eberstadt for help with initial measurements and R. Peteranderl and T. Diercks for helpful discussions. We also thank R. Gschwind and T. Diercks for sharing their pulse programs. M. C. gratefully acknowledges the financial support of the *Alexander von Humboldt-Stiftung*.

REFERENCES

1. Hendrickson, W. A. & Wüthrich, K. (1996) *Macromolecular structures*, Current Biology, London.
2. Oschkinat, H., Mueller, T. & Dieckmann, T. (1994) Protein structure determination with three- and four-dimensional NMR spectroscopy, *Angew. Chem. Int. Ed. Engl. 33*, 277−293.
3. Sattler, M. & Fesik, S. W. (1996) Use of deuterium labeling in NMR: overcoming a sizeable problem, *Structure 4*, 1245−1249.
4. Girvin, M. E. & Fillingame, R. H. (1993) Helical structure and folding of subunit c of F_1F_0 ATP synthase: ^1H NMR resonance assignments and NOE analysis, *Biochemistry 32*, 12167−12177.
5. Girvin, M. E. & Fillingame, R. H. (1994) Hairpin folding of subunit c of F_1F_0 ATP synthase: ^1H distance measurements to nitroxide-derivatized aspartyl-61, *Biochemistry 33*, 665−674.
6. Girvin, M. E. & Fillingame, R. H. (1995) Determination of local protein structure by spin-label difference 2D NMR: the region neighboring Asp61 of subunit c of F_1F_0 ATP synthase, *Biochemistry 34*, 1635−1645.
7. Fillingame, R. H. (1996) Membrane sectors of F- and V-type H^+-transporting ATPases, *Curr. Opin. Struct. Biol. 6*, 491−498.
8. Williams, K. A., Farrow, N. A., Deber, C. M. & Kay, L. E. (1996) Structure and dynamics of bacteriophage IKe major coat protein in MPG micelles by solution NMR, *Biochemistry 35*, 5145−5157.
9. Pervushin, K. V., Orekhov, V. Y., Popov, A. I., Musinda, L. Y. & Arseniev, A. S. (1994) Three-dimensional structure of (1-71) bacterioopsin solubilized in methanol/chloroform and SDS micelles determined by ^{15}N-^1H heteronuclear NMR spectroscopy, *Eur. J. Biochem. 219*, 571−583.
10. Orekhov, V. Y., Abdulaeva, G. V., Musina, L. Y. & Arseniev, A. S. (1992) ^1H-^{15}N-NMR studies of bacteriorhodopsin *Halobacterium halobium*, *Eur. J. Biochem. 210*, 223−229.
11. Henry, G. D. & Sykes, B. D. (1994) Methods to study membrane protein structure in solution, *Methods Enzymol. 239*, 515−535.
12. Opella, S. J., Kim, Y. & McDonnel, P. (1994) Experimental nuclear magnetic resonance studies of membrane proteins, *Methods Enzymol. 239*, 536−560.
13. Vinogradova, O., Badola, P., Czerski, L., Sönnichsten, F. D. & Sanders, C. R. II (1997) *Escherichia coli* diacylglycerol kinase: a case study in the application of solution NMR methods to an integral membrane protein, *Biophys. J. 72*, 2688−2701.
14. Bechinger, B. & Opella, S. J. (1991) Flat-coil probe for NMR-spectroscopy of oriented membrane samples, *J. Magn. Reson. 95*, 585−588.
15. Marassi, F. M., Ramamoorthy, A. & Opella, S. J. (1997) Complete resolution of the solid-state NMR spectrum of a uniformly ^{15}N-labeled membrane protein in phospholipid bilayers, *Proc. Natl Acad. Sci. USA 94*, 8551−8556.
16. Sanders, C. R., Hare, B. J., Howard, K. & Prestegard, J. H. (1993) Magnetically-oriented phospholipid micelles as a tool for the study of membrane-associated molecules, *Prog. NMR Spectrosc. 26*, 421−444.
17. Prosser, R. S., Hunt, S. A., DiNatale, J. A. & Vold, R. R. (1996) Magnetically aligned membrane model systems with positive order parameter: switching the sign of S_{zz} with paramagnetic ions, *J. Am. Chem. Soc. 118*, 269−270.
18. Howard, K. P. & Opella, S. J. (1996) High-resolution solid-state NMR spectra of integral membrane proteins reconstituted into magnetically oriented phospholipid bilayers, *J. Magn. Reson. 112*, 91−94.
19. Opella, S. (1997) NMR and membrane proteins, *Nat. Struct. Biol. NMR Suppl.*, 845−848.
20. Schuldiner, S., Lebendiker, M. & Yerushalmi, H. (1997) EmrE, the smallest ion-coupled transporter, provides a unique paradigm for structure-function studies, *J. Exp. Biol. 200*, 335−341.

21. Yerushalmi, H., Lebendiker, M. & Schuldiner, S. (1995) EmrE, an *Escherichia coli* 12-kDa multidrug transporter, exchanges toxic cations and H^+ and is soluble in organic solvents, *J. Biol. Chem. 70*, 6856−6863.
22. Lebendiker, M. & Schuldiner, S. (1996) Identification of residues in the translocation pathway of EmrE, a multidrug antiporter from *Escherichia coli*, *J. Biol. Chem. 271*, 31 044−31 048.
23. Arkin, I. T., Russ, W. P., Lebendiker, M. & Schuldiner, S. (1996) Determining the secondary structure and orientation of EmrE, a multi-drug transporter, indicates a transmembrane four-helix bundle, *Biochemistry 35*, 7233−7238.
24. Schägger, H. & von Jagow, G. (1987) Tricine-SDS/PAGE for the separation of proteins in the range from 1 to 100 kDa, *Anal. Biochem. 166*, 368−379.
25. Peterson, G. (1977) A simplification of the protein assay method of Lowry et al. which is more generally applicable, *Anal. Biochem. 83*, 346−356.
26. Wishart, D. S., Bigham, C. G., Holm, A., Hodges, R. S. & Sykes, B. D. (1995) ^{1}H, ^{13}C and ^{15}N random coil NMR chemical shifts of the common amino acids. I. Investigation of nearest-neighbor effects, *J. Biomol. NMR 6*, 67−81.
27. Palmer, A. G. III, Cavanagh, J., Wright, P. E. & Rance, M. (1991) Sensitivity improvement in proton-detected two-dimensional heteronuclear correlation NMR spectroscopy, *J. Magn. Reson. 93*, 151−170.
28. Kay, L. E., Keifer, P. & Saarinen, T. (1992) Pure absorption gradient enhanced heteronuclear single quantum correlation spectroscopy with improved sensitivity, *J. Am. Chem. Soc. 114*, 10 663−10 665.
29. Maudsley, A. A., Wokaun, A. & Ernst, R. R. (1978) Coherence transfer echoes, *Chem. Phys. Lett. 55*, 9−14.
30. Hurd, R. E. & John, B. K. (1991) Gradient-enhanced proton-detected heteronuclear multiple-quantum coherence spectroscopy, *J. Magn. Reson. 91*, 648−653.
31. Powers, R., Gronenbom, A. M., Clore, G. M. & Bax, A. (1991) Three-dimensional triple-resonance NMR of ^{13}C/^{15}N-enriched proteins using constant-time evolution, *J. Magn. Reson. 94*, 209−213.
32. Grzesiek, S. & Bax, A. (1993) The importance of not saturating H_2O in protein NMR. Application to sensitivity enhancement and NOE measurements, *J. Am. Chem. Soc. 115*, 12 593−12 594.
33. Marion, D., Driscoll, P. C., Kay, L. E., Wingfield, P. T., Bax, A., Gronenbom, A. M. & Clore, G. M. (1989) Overcoming the overlap problem in the assignment of ^{1}H NMR spectra of larger proteins by use of three-dimensional heteronuclear ^{1}H-^{15}N Hartmann-Hahn-multiple quantum coherence and nuclear overhauser-multiple quantum coherence spectroscopy: application to interleukin 1*β*, *Biochemistry 28*, 6150−6156.
34. Shaka, A. J., Keeler, J., Frenkiel, T. & Freeman, R. (1983) An improved sequence for broadband decoupling: WALTZ-16, *J. Magn. Reson. 52*, 335−338.
35. Zuiderweg, E. R. P. & Fesik, S. W. (1989) Heteronuclear three-dimensional NMR spectroscopy of the inflammatory protein C5a, *Biochemistry 28*, 2387−2391.
36. Marion, D., Kay, L. E., Sparks, S. W., Torchia, D. A. & Bax, A. (1989) Three-dimensional heteronuclear NMR of ^{15}N-labeled proteins, *J. Am. Chem. Soc. 111*, 1515−1517.
37. Vuister, G. W. & Bax, A. (1993) Quantitative J correlations: a new approach for measuring homonuclear three-bond $J(H^nH^\alpha)$ coupling constants in ^{15}N-enriched proteins, *J. Am. Chem. Soc. 115*, 7772−7777.
38. Archer, S. J., Ikura, M., Sporn, M. B., Torchia, D. A. & Bax, A. (1991) An alternative 3D NMR technique for correlating backbone ^{15}N with side H*β* resonances in larger proteins, *J. Magn. Reson. 95*, 636−641.
39. Grzesiek, S. & Bax, A. (1992) Improved 3D Triple-resonance NMR techniques applied to a 31 kDa protein, *J. Magn. Reson. 96*, 432−440.
40. Kay, L. E., Xu, G., Singer, A. U., Muhandiram, D. R. & Forman-Kay, J. D. (1993) A gradient-enhanced HCCH-TOCSY experiment for recording side-chain ^{1}H and ^{13}C correlations in H_2O samples of proteins, *J. Magn. Reson. 101*, 333−337.
41. Farmer, B. T. II & Venters, R. A. (1995) Assignment of side-chain ^{13}C resonances in perdeuterated proteins, *J. Am. Chem. Soc. 111*, 4187−4188.
42. Gschwind, R., Gemmecker, G. & Kessler, H. (1998) A spin system labeled and highly resolved ed-H(CCO)NH-TOCSY experiment for the facilitated assignment of proton side-chains in partially deuterated samples, *J. Biomol. NMR*, in the press.
43. Piotto, M., Saudek, V. & Sklenár, V. J. (1992) Gradient-tailored excitation for single-quantum NMR spectroscopy of aqueous solutions, *J. Biomol. NMR 2*, 661−665.
44. Barbato, G., Ikura, M., Kay, L. E., Pastor, R. W. & Bax, A. (1992) Backbone dynamics of Calmodulin studied by ^{15}N relaxation using inverse detected two-dimensional NMR spectroscopy: the central helix is flexible, *Biochemistry 31*, 5269−5278.
45. Fillingame, R. H. (1976) Purification of the carbodiimide-reactive protein component of the ATP energy-transducing system of *Escherichia coli*, *J. Biol. Chem. 251*, 6630−6637.
46. Wüthrich, K. (1986) *NMR of proteins and nucleic acids*, Wiley, New York.
47. Bundi, A. & Wüthrich, K. (1979) ^{1}H-NMR parameters of the common amino acid residues measured in aqueous solutions of the linear tetrapeptides H-Gly-Gly-X-L-Ala-OH, *Biopolymers 18*, 285−297.
48. Wishart, D. S., Bigham, C. G., Yao, J., Abildgaard, F., Dyson, H. J., Oldfield, E., Manley, J. L. & Sykes, D. (1995) ^{1}H, ^{13}C and ^{15}N chemical shift referencing in biomolecular NMR, *J. Biomol. NMR 6*, 135−140.
49. Reference deleted.
50. Henry, G. D. & Sykes, B. D. (1992) Assignment of amide ^{1}H and ^{15}N NMR resonances in detergent-solubilized M13 coat protein: a model for the coat protein dimer, *Biochemistry 31*, 5284−5297.
51. MacKenzie, K. R., Prestegard, J. H. & Engelman, D. M. (1997) A transmembrane helix dimer: structure and implications, *Science 276*, 131−133.
52. Lou, P. & Baldwin, R. L. (1997) Mechanism of helix induction by trifluoroethanol: a framework for extrapolating the helix-forming properties of peptides from trifluoroethanol/water mixtures back to water, *Biochemistry 36*, 8413−8421.
53. Buck, M., Schwalbe, H. & Dobson, C. M. (1995) Characterization of conformational preferences in a partly folded protein by heteronuclear NMR spectroscopy: assignment and secondary structure analysis of hen egg-white Lysozyme in trifluoroethanol, *Biochemistry 34*, 13 219−13 232.
54. Pervushin, K. V. & Arseniev, A. S. (1992) Three-dimensional structure of (1-36)bacterioopsin in methanol-chloroform mixture and SDS micelles determined by 2D ^{1}H-NMR spectroscopy, *FEBS Lett. 308*, 190−196.
55. Gesell, J., Zasloff, M. & Opella, S. J. (1997) Two-dimensional ^{1}H NMR experiments show that the 23-residue magainin antibiotic peptide is an *α*-Helix in dodecylphoshocholine micelles, sodium dodecylsulfate micelles, and triflourethanol/water solution, *J. Biomol. NMR 9*, 127−135.
56. Gratias, R. & Kessler, H. (1998) Molecular dynamics study on microheterogeneity and preferential solvation in methanol/chloroform mixtures, *J. Phys. Chem.*, in the press.
57. Nozaki, Y., Reynolds, J. A. & Tanford, C. (1978) Conformational states of a hydrophobic protein. The coat protein of fd bacteriophage, *Biochemistry 17*, 1239−1246.
58. Diercks, T., Schwaiger, M. & Kessler, H. (1998) HSQC-based methyl group selection via gradients in multidimensional NMR spectroscopy of proteins, *J. Magn. Reson. 130*, 335−340.
59. Mulder, F. A. A., Spronk, C. A. E. M., Slijper, M., Kaptein, R. & Boelens, R. (1996) Improved HSQC experiments for the observation of exchange broadened signals, *J. Biomol. NMR 8*, 223−228.

Supplementary material. **Table S1. Backbone and sidechain ^{15}N, ^{1}H and ^{13}C chemical shifts of EmrE.** This information is available, on request, from the Editorial Office. Eight pages are available. Chemical shift values were deposited in the BioMagRes database in account 4136.